

RESEARCH ARTICLE

Study of Welding Dissimilar Metals – Low-carbon Steel AISI 1018 and Austenitic Stainless Steel AISI 304

Younis K. Khdir¹, Salim A. Kako², Ramadhan H. Gardi³

¹Department of Mechanic and Energy Engineering, College of Technical Engineering, Erbil Polytechnic University, Erbil, Kurdistan Region, Iraq, ²Department of Mechanic, Technical Institute, Erbil Polytechnic University, Erbil, Kurdistan Region, Iraq, ³Department of Mechanic and Mechatronic, College of Engineering, Salahaddin University, Erbil, Kurdistan Region, Iraq

***Corresponding author:**

Younis K. Khdir, Department of Mechanic and Energy Engineering, College of Technical Engineering, Erbil Polytechnic University, Erbil, Kurdistan Region, Iraq.
E-mail: younis.khdir@epu.edu.iq

Received: 07 January 2020

Accepted: 07 June 2020

Published: 30 June 2020

DOI

10.25156/ptj.v10n1y2020.pp1-5

ABSTRACT

The aim of this study is to investigate the influence of different heat inputs on mechanical properties and microstructure of dissimilar electrical arc welded austenitic stainless steel AISI 304 and low-carbon steel (CS) joints. The mechanical properties of welded austenitic stainless steel type AISI 304 and low-CS are studied. Five different heat inputs 0.5, 0.9, 1.41, 2, and 2.5 KJ/min were applied to investigate the microstructure of the welded zone and mechanical properties. The results showed that the efficiency of the joints and tensile strength increased with increasing heat inputs, while excess heat input reduces the efficiency. Furthermore, changes in microstructure with excess heat input cause failure at the heat-affected zone.

Keywords: Arc welding; AISI 304; Low-carbon steel AISI 1018; Hardness tests; Dissimilar weld joint

INTRODUCTION

Welding low-carbon steel (CS) AISI 1018 and stainless steel 304 are used in various engineering applications such as coal mining industries, power plant, petrochemical, automobiles, pipelines, submarine environments, construction materials, and aerospace engineering for the reasons of quality, performance and reducing the production cost (Chen et al., 2017, Yang et al., 2017). Studies (Bodude and Momohjimoh, 2015, Muthupandi et al., 2003, Yang et al., 2012) show that the microstructure and the mechanical properties are affected by the amount of the heat input that is applied during the welding process. The dissimilar metal joints between austenitic stainless steel and low-CS have many critical applications in different fields of industry, such as in boilers, pressure vessels, and heat exchangers of power plants and other industries such as petrochemical, oil, and gas industry (Pouraliakbar et al., 2014).

Mani et al., 2015, characterized the microstructure of dissimilar welded components AISI 304 austenitic and AISI 430 ferritic stainless steel (FSS) alloys. The results indicated that the width of welding zone and heat-affected zone (HAZ) became much thinner depending on the increased welding speed. On the other hand, the width becomes wider depending on the increased heat input. Moharana

et al., 2016, investigated the mechanical properties and microstructure of austenitic stainless steel and Cu. The study confirmed the well mixing of stainless steel and Cu inside the weld pool. They found that the tensile stress up to 201 MPa can be obtained and they noticed that the fracture occurred outside the weld zone.

Bodude and Momohjimoh, 2015, studied the effects of welding parameters on the mechanical properties of welded low-CS, they found that the tensile strength and hardness decrease with increasing the heat input. Jafarzadegan et al., 2013, studied the microstructure and mechanical properties of a dissimilar friction Stir Weld between Austenitic Stainless Steel and Low-CS. They noticed that in the stir zone of st37 steel, the hot deformation of the material in the austenite region produced small austenite grains. These grains transformed into fine ferrite and pearlite by cooling the material after friction stir welding. The production of fine grains increases the hardness and tensile strength in the stir zone of both sides with respect to their base metals.

Singh et al., 2016, showed the effect of post-weld heat treatment (PWHT) on friction welded joint of CS to stainless steel, they concluded that the tensile strength and elongation of the joint were improved substantially after PWHT at 400°C, which could reach up to the equivalent strength of stainless steel and elongation of CS. They

showed that these results attributed to microstructural changes which become more homogeneous and the amount of chromium carbides barely increased, while the fracture mode also altered from quasi-cleavage fracture in the as-welded joint to the combination of dimple fracture and quasi-cleavage fracture after PWHT. Wu et al., 2015, studied the correlation between microstructure, mechanical properties, and corrosion-resistant of laser welded dissimilar joints between FSS and CS. They noticed that the joints with different welding speed have similar ultimate tensile strength but with superior elongation. Related to the electrochemical corrosion test, they reported the corrosion potential of dissimilar joints falls between FSS and CS.

Paventhan et al., 2012, studied the optimization of friction welding process parameters for joining CS and stainless steel; they performed response surface methodology to optimize the friction welding process parameters to attain maximum tensile strength of the joint. They concluded that the maximum tensile strength of 543 MPa can be obtained for the joints fabricated under the welding conditions of friction pressure of 90 MPa, forging pressure of 90 MPa, friction time of 6 s, and forging time of 6 s.

The significance of this paper is although a large number of researches on dissimilar welded joints have been done, till now, the information about dissimilar weld between AISI 304 and CS is very scarce. The aim of this research is studying the influence of different heat inputs on mechanical properties and microstructure of dissimilar electrical arc welded austenitic stainless steel 304 and low steel CS joints.

EXPERIMENTAL PROCEDURE

Austenitic stainless steel type AISI 304 and low-CS AISI 1018 type with 3 mm sheet thickness, 30 mm width, and 80 mm length are used. The chemical composition and the mechanical properties of the materials are shown in Tables 1 and 2, respectively. The microstructures of both materials are showed in Figures 1 and 2.

Automatic GMB weld was used to weld the dissimilar materials in this study. To produce welds, the two materials are welded in butt joint configuration. Filler metal wires, with the composition shown in Table 3, are used. So as to test the heat input effects on the metallurgical aspects of the welded zone, different applied voltage, current, and torch speed are selected to achieve on different heat inputs, which were 0.5, 0.9, 1.4, 2, and 2.5 KJ/mm.

Figure 3 shows that the welded samples were prepared for the tensile test standard ASTM E8M-04 by removing

Table 1: Chemical composition of base metals

Materials	Cr%	Ni%	C%	Mo%	Mn%	P%	Si%	S%	Fe
AISI 304	18.33	8.33	0.03	0.2	1.48	0.03	0.58	0.01	Bal.
AISI 1018	0.05	0.06	0.14	0.001	0.92	0.01	0.24	0.014	Bal.

Table 2: Mechanical properties of the materials

Materials	Yield strength MPa	Tensile strength MPa	Ultimate tensile strength MPa	Fracture strength MPa
AISI 304	340	345	650	294
AISI 1018	250	258	340	240

Table 3: Composition of filler materials weight percentage

Materials	C	Si	Mn	Ni	Cr
Electrode wire	0.11	0.9	0.5–2.5	12.0–14.0	22.0–25.0

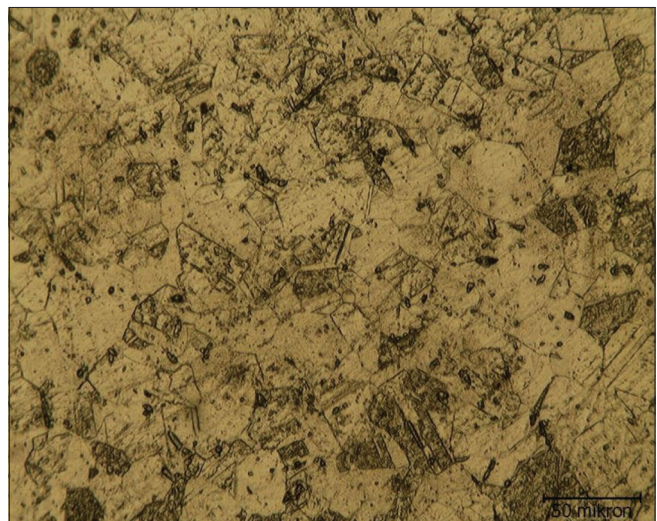


Figure 1: Microstructure of stainless steel AISI 304 as received



Figure 2: Microstructure of as received low-carbon steel AISI 1018(x600)

extra materials from the gauge length using the milling and shaper machines

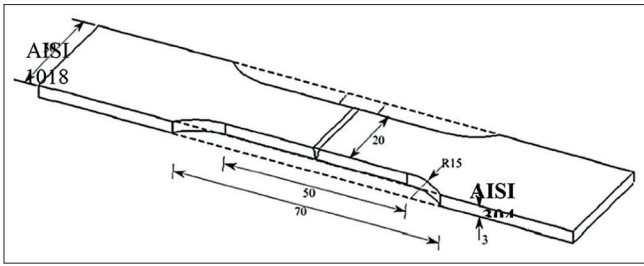


Figure 3: Schematic diagram of welding specimen

Tensile tests were conducted on the welded steel samples using a hydraulic extensometer.

The joint efficiency is measured according to equation no. 1

$$\text{Efficiency of Joint} = \frac{\text{Tensile strength of welded joint}}{\text{Tensile strength of softer metal}} \times 100 \quad (1)$$

The heat inputs are calculated with equation no. 2:

$$\text{Heat input (HI)} = \frac{\text{Voltage (V)} \times \text{Current (I)}}{\text{Velocity} \frac{(v) \text{ mm}}{\text{s}}} \times 100 \quad (2)$$

Where; HI = welded heat input, I = welding current intensity, V = welding voltage and v = welding velocity.

After the process, the samples were ground to a 220, 500, 600, 800, and 1000-grit, respectively, and subsequently polished with 0.3 μm Al₂O₃ diamond paste. For the microstructural test, the specimens etched chemically according to ASTM standard. The solution for low-CS is Nital, consist of 98% distilled water and 2% HNO₃ and etching time equals to 15 s, while for austenitic stainless steel, the solution consists of a saturated solution of FeCl₃ in HCl to which a little HNO₃ is added and etching time equals to 5 min. Metallographic examinations of butt and groove welds were performed using optical microscope Olympus PMG3 with magnification × 600.

RESULTS AND DISCUSSION

Figure 4 shows stress–strain curves for base materials. Noticed that the values of yield strength, ultimate tensile strength, and fracture strength of austenitic stainless steel AISI 304 is higher than low-carbon steel AISI 1018 due to austenitic phase and presents of higher percentage of different elements such as Ni, Cr, and Mn, the austenitic phase can be shown in Figures 1 and 2.

Figure 5 shows the relationship between different heat inputs and different mechanical properties for the dissimilar welded specimens between austenitic stainless steel and

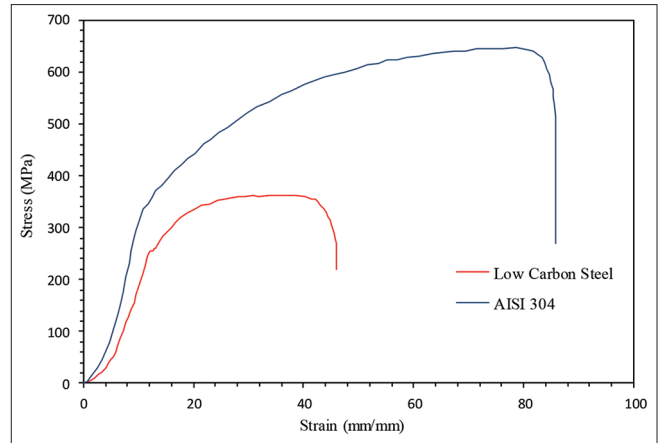


Figure 4: Stress–strain curve for as received AISI 304 and low-carbon steel AISI 1018

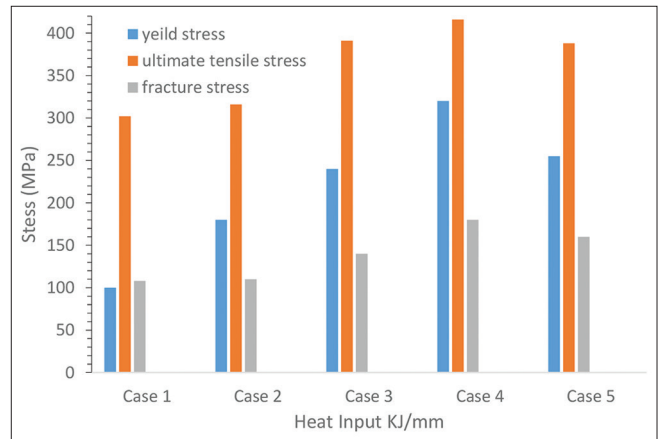


Figure 5: Effect of heat input on the mechanical properties shows the relationship between the stress and different heat inputs

low-CS. The figure shows that at low heat input 0.5 KJ/min, the tensile strength of welded specimen is 300 MPa and fracture stress is 108 MPa, with increasing the heat input the ultimate tensile strength gradually and reached to their maximum values 416 when heat input equals to 2 KJ/min, increasing the heat input further to 2.5 KJ/min, the behavior of welded specimens showed reduction in mechanical properties and reduce to 388 MPa and 160 MPa for both ultimate tensile strength and fracture strength, respectively. The results attributed to solid solution formation between two base material and electrode material, while excess heat inputs cause reducing these values. Figures 6 and 7 exhibit this phenomenon.

The fractured specimens showed that the fracture occurs at heat-affected zone at different heat inputs from 0.5 KJ/min to 2 KJ/min, while at excessive heat input 2.5 KJ/min, the fracture occurred at weld zone. Figure 6 shows insufficient melting between the two metals and formation of the solid solution and insufficient welding joint.

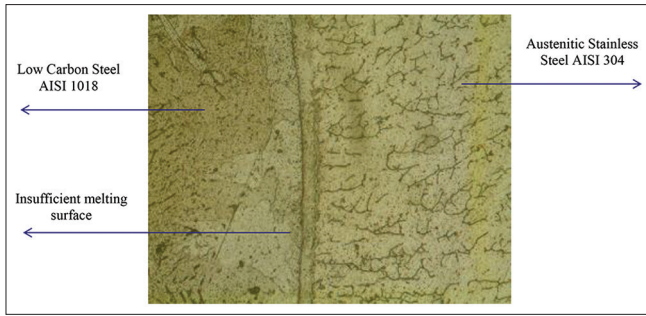


Figure 6: Weld joint at heat input 0.5 KJ/min (x600)

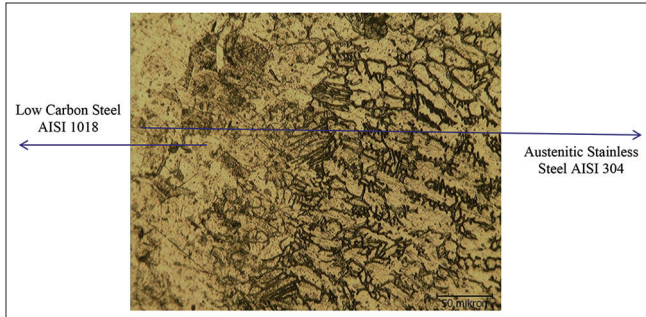


Figure 7: Fracture of weld joint at diffusion zone at heat input 0.9 KJ/min (x600)

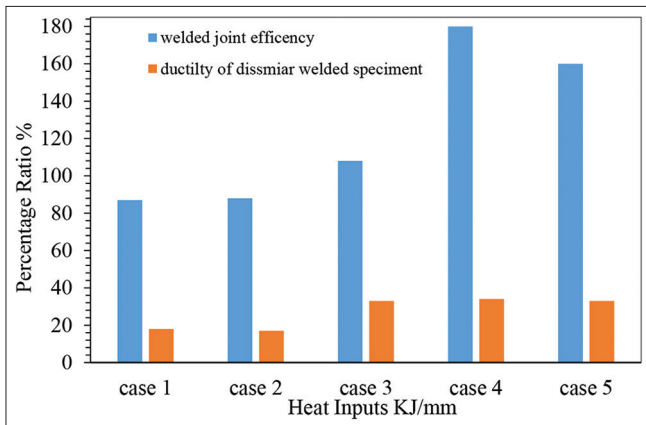


Figure 8: Relation between weld joint efficiency and elongation ratio with heat inputs

The microstructures showed that with increasing the heat input the amount of delta ferrite in weld zone increased, and also, grain growth can be seen at heat-affected zone at both sides of the weld lines, as shown in Figure 7. Figure 8 increasing efficiency of welded joints and the elongation of dissimilar welded material with increasing heat input.

Hardness testing of all the specimen (both sides, Haz location, and welding joints) was performed in accordance with ASTM E92-17 standard using Vickers Testing Machine of metallic materials. The samples of the specimens were placed with the surface on the anvil, and slowly turning the handwheel until the specimen was raised to touch the

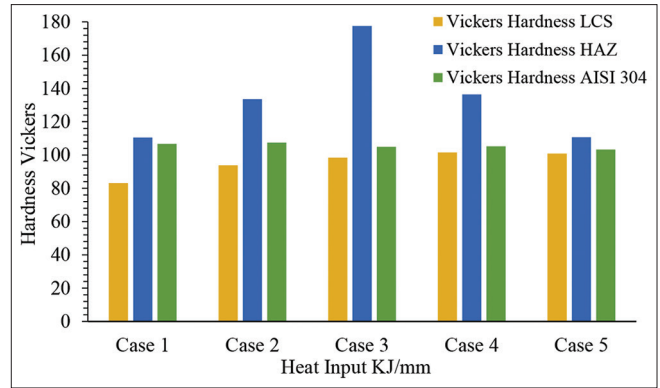


Figure 9: Relation between Vickers hardness of base materials and heat-affected zone zones with heat inputs

indenter. The numbers were read directly from the dial indicator and converted to the Vickers number.

Hardness test was done in a row to ensure that the base material, HAZ, and weld metal at a distance ≤ 2 mm from the surface and 2 mm from fusion line were captured. Schematic representation of Butt and Groove welded joint with the locations of hardness testing and examination of the microstructure is shown in Figure 9.

CONCLUSION

In this study, microstructural properties and efficiency of dissimilar welded joints of (low-CS – AISI 304) with arc welding were analyzed and these results were obtained.

- 1) Low-CS AISI 1018 can be joined with austenitic stainless steel AISI 304 by arc welding.
- 2) During tensile strength tests, we observed that fractures were close to low-CS side.
- 3) After welding, it was observed that the values of tensile strengths of the joints increased due to the formation of the solid solution state in the fusion zone.
- 4) It was observed that the fusion zone was, on average about $\sim 1-2$ mm in width, the deep penetration was on average ~ 3 mm in depth.
- 5) The best properties in terms of microstructure, elongation, and tensile test were observed at the specimen bonded at heat input at 2 KJ/min.

REFERENCES

- Bodude, M. and I. Momohjimoh. 2015. Studies on effects of welding parameters on the mechanical properties of welded low-carbon steel. *J. Miner. Mater. Charact. Eng.* 3: 142.
- Chen, Y. W., B. M. Huang, Y. T. Tsai, S. P. Tsai, C. Y. Chen and J. R. Yang. 2017. Microstructural evolutions of low carbon Nb/Mo-containing bainitic steels during high-temperature tempering. *Mater. Charact.* 131: 298-305.
- Jafarzadegan, M., A. Abdollah-Zadeh, A. Feng, T. Saeid, J. Shen and

- H. Assadi. 2013. Microstructure and mechanical properties of a dissimilar friction stir weld between austenitic stainless steel and low carbon steel. *J. Mater. Sci. Technol.* 29: 367-372.
- Mani, A. A., T. S. Kumar and M. Chandrasekar. 2015. Mechanical and metallurgical properties of dissimilar welded components (AISI 430 ferritic-AISI 304 austenitic stainless steels) by CO₂ laser beam welding (LBW). *J. Chem. Pharm. Sci.* 974: 2115.
- Moharana, B. R., S. K. Sahu, S. K. Sahoo and R. Bathe. 2016. Experimental investigation on mechanical and microstructural properties of AISI 304 to Cu joints by CO₂ laser. *Eng. Sci. Technol. Int. J.* 19: 684-690.
- Muthupandi, V., P. B. Srinivasan, S. Seshadri and S. Sundaresan. 2003. Effect of weld metal chemistry and heat input on the structure and properties of duplex stainless steel welds. *Mater. Sci. Eng. A.* 358: 9-16.
- Paventhana, R., P. Lakshminarayanan and V. Balasubramanian. 2012. Optimization of friction welding process parameters for joining carbon steel and stainless steel. *J. Iron Steel Res. Int.* 19: 66-71.
- Pouraliakbar, H., M. Hamed, A. H. Kokabi and A. Nazari. 2014. Designing of CK45 carbon steel and AISI 304 stainless steel dissimilar welds. *Mater. Res.* 17: 106-114.
- Singh, R., R. Kumar, L. Feo and F. Fraternali. 2016. Friction welding of dissimilar plastic/polymer materials with metal powder reinforcement for engineering applications. *Compos. Part B Eng.* 101: 77-86.
- Wu, W., S. Hu and J. Shen. 2015. Microstructure, mechanical properties and corrosion behavior of laser welded dissimilar joints between ferritic stainless steel and carbon steel. *Mater. Des.* 65: 855-861.
- Yang, D., X. Li, D. He, H. Huang and L. Zhang. 2012. Study on microstructure and mechanical properties of Al-Mg-Mn-Er alloy joints welded by TIG and laser beam. *Mater. Des.* 40: 117-123.
- Yang, W., W. Liu, Z. Peng, B. Liu and J. Liang. 2017. Characterization of plasma electrolytic oxidation coating on low carbon steel prepared from silicate electrolyte with Al nanoparticles. *Ceram. Int.* 43: 16851-16858.